


**Please cite the Published Version**

Garcia Martin, LM, Blake, T, Brook, N , Cicala, MF, Cussans, D, van Dijk, MWU, Forty, R, Gershon, T, Gys, T, Hadavizadeh, T, Harnew, N, Jones, T, Kreps, M, Rademacker, J, Smallwood, JC and Tat, M (2023) TORCH pattern recognition and particle identification performance. Nuclear Instruments and Methods in Physics Research Section A: Accelerators, Spectrometers, Detectors, and Associated Equipment, 1055. p. 168437. ISSN 0168-9002

**DOI:** <https://doi.org/10.1016/j.nima.2023.168437>

**Publisher:** Elsevier

**Version:** Published Version

**Downloaded from:** <https://e-space.mmu.ac.uk/632360/>

**Usage rights:**  [Creative Commons: Attribution 4.0](https://creativecommons.org/licenses/by/4.0/)

**Additional Information:** This is an Open Access article published in Nuclear Instruments and Methods in Physics Research Section A: Accelerators, Spectrometers, Detectors, and Associated Equipment, by Elsevier.

**Enquiries:**

If you have questions about this document, contact [openresearch@mmu.ac.uk](mailto:openresearch@mmu.ac.uk). Please include the URL of the record in e-space. If you believe that your, or a third party's rights have been compromised through this document please see our Take Down policy (available from <https://www.mmu.ac.uk/library/using-the-library/policies-and-guidelines>)



# TORCH pattern recognition and particle identification performance

L.M. Garcia Martin<sup>a,\*</sup>, T. Blake<sup>a</sup>, N.H. Brook<sup>b</sup>, M.F. Cicala<sup>a</sup>, D. Cussans<sup>c</sup>, M.W.U. van Dijk<sup>d</sup>,  
R. Forty<sup>d</sup>, T. Gershon<sup>a</sup>, T. Gys<sup>d</sup>, T. Hadavizadeh<sup>e</sup>, N. Harnew<sup>e</sup>, T. Jones<sup>a</sup>, M. Kreps<sup>a</sup>,  
J. Rademacker<sup>c</sup>, J.C. Smallwood<sup>e</sup>, M. Tat<sup>e</sup>

<sup>a</sup> Department of Physics, University of Warwick, Coventry, United Kingdom

<sup>b</sup> University of Bath, Claverton Down, Bath, United Kingdom

<sup>c</sup> H.H. Wills Physics Laboratory, University of Bristol, Bristol, United Kingdom

<sup>d</sup> European Organisation for Nuclear Research (CERN), Geneva, Switzerland

<sup>e</sup> Denys Wilkinson Laboratory, University of Oxford, Oxford, United Kingdom

## ARTICLE INFO

### Keywords:

Particle identification

Time-Of-Flight detectors

## ABSTRACT

The TORCH detector aims to provide  $K/\pi$  ( $K/p$ ) separation up to a momentum of about 10 (15) GeV/ $c$  by measuring their time-of-flight at the LHCb detector. Prompt Cherenkov photons are produced in a quartz radiator bar of 10 mm thickness, and propagated via total internal reflection to the periphery of the detector, where they are focused onto an array of microchannel plate photomultipliers that measure the photon arrival time and position. Pattern recognition techniques are used to compare the likelihood that the detector image is due to a given particle hypothesis. Good performance is obtained even for very high detector occupancies.

## 1. Introduction

The excellent Particle IDentification (PID) capability of the LHCb experiment has been crucial for the success of its physics programme. Such PID capabilities are provided by two Ring Imaging Cherenkov (RICH) detectors [1]. However, with the existing RICH detectors, kaons (protons) below 10 (15) GeV/ $c$  fall below the Cherenkov threshold and cannot be positively separated from pions.

The Time Of internally Reflected Cherenkov (TORCH) detector is a proposed large-area Time-Of-Flight (TOF) detector, which aims to enhance the PID performance of the LHCb detector in the 2–15 GeV/ $c$  momentum range [2]. TORCH exploits the difference in TOF between several species of particles with the same momentum. Prompt Cherenkov photons are radiated when charged hadrons traverse a 10 mm-thick quartz plate. The Cherenkov photons are propagated, via total internal reflection, to the periphery of the radiator, where a cylindrical mirrored surface focuses them onto an array of fast-timing photon detectors. The cylindrical mirror is designed such that the  $y$  position (height) in the MCP can be mapped to the entry angle of the photon in the focusing block, while in the  $x$  direction, the photon is just reflected. Fig. 1 shows a side view of TORCH with the possible path of a Cherenkov photon emitted by a charged hadron. The full detector will comprise 18 optically isolated modules, each with a quartz radiator of 2.5 m height, 66 cm width and 1 cm depth, and a focusing block. The 18 radiator bars will cover an area of  $5 \times 6 \text{ m}^2$ . TORCH will be installed in front of RICH2 of LHCb, at  $\sim 9.5 \text{ m}$  from the  $pp$  interaction point.

The TORCH installation is now included in the Upgrade II plans for the LHCb experiment [3]. Given the flight path of particles detected by TORCH, the difference in TOF between kaons and pions at a momentum of 10 GeV/ $c$  is around 35 ps. Achieving a statistical separation of  $3\sigma$  will require a time precision of 10–15 ps per-track. Given 20–30 photons are expected to be detected per-track, the desired per-track time resolution translates to a time resolution of about 70 ps for single photons. Such resolution depends on accurate time measurements but also on precise spatial measurements to have an accurate reconstruction. These features are provided by microchannel plate photomultipliers (MCP-PMT) [4], with  $64 \times 8$  pixels covering an active area of  $53 \times 53 \text{ mm}^2$ . Exploiting charge-sharing, photons can be reconstructed as a cluster instead of as a single pixel and an effective granularity of  $128 \times 8$  is achieved. Such granularity grants an angular resolution of  $\sim 1 \text{ mrad}$  in the  $x$ - and  $y$ -directions.

## 2. Reconstruction

The Cherenkov light pattern in TORCH is a three-dimensional image (in space and time), which is folded by reflections from the sides of the module. An example image is shown in Fig. 2.

The photon detectors measure the arrival time ( $t_{\text{arrival}}$ ) and position of the photons which can then be used to calculate the azimuthal ( $\phi_C$ ) and polar ( $\theta_C$ ) Cherenkov angles of the emitted photon, and the photon path length in the radiator. The arrival time on the photon detector

\* Corresponding author.

E-mail address: [luis.miguel.garcia.martin@cern.ch](mailto:luis.miguel.garcia.martin@cern.ch) (L.M. Garcia Martin).

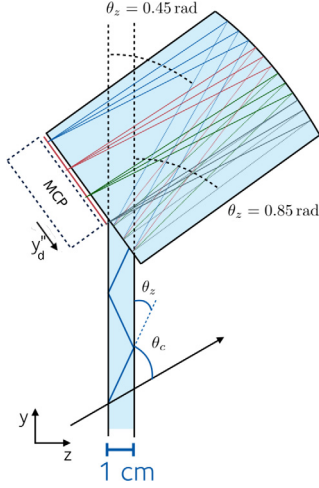


Fig. 1. Side view of one TORCH module showing how a Cherenkov photon, when emitted by a charged hadron in the quartz radiator, propagates to the periphery of the detector via total internal reflection. Cherenkov photons are focused onto an array photon detectors by a cylindrical mirror at the very edge of the focusing block. Different wavelengths of light will be emitted with different Cherenkov angles and will be focused into different positions on the MCP by the mirror.

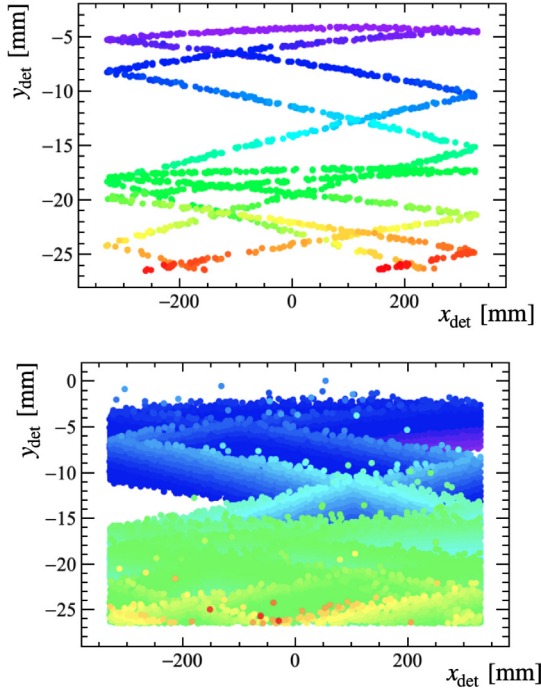


Fig. 2. Expected TORCH image on the detector plane for a single charged particle, (top) without chromatic dispersion and (bottom) with chromatic dispersion. The colour indicates the arrival time of the photon from (purple) earliest to (red) latest. The photon yield has been artificially increased to demonstrate the pattern. The folds in the pattern are due to the reflections in the side of the module. Reflections from the bottom of the bar also appear ‘disconnected’ from the pattern.

plane, and the photon time of propagation, can be used to infer the TOF of the hadron,

$$t_{\text{arrival}} = t_0 + t_{\text{TOF}} + t_{\text{prop}}. \quad (1)$$

Here, the production time,  $t_0$ , indicates when the charged hadron is created. The particle flies for a time,  $t_{\text{TOF}}$ , before emitting a Cherenkov photon inside TORCH, and that photon propagates for time  $t_{\text{prop}}$  before reaching the photon detectors. The TOF can be disentangled from  $t_{\text{arrival}}$  using information from the tracking system. The production time can be

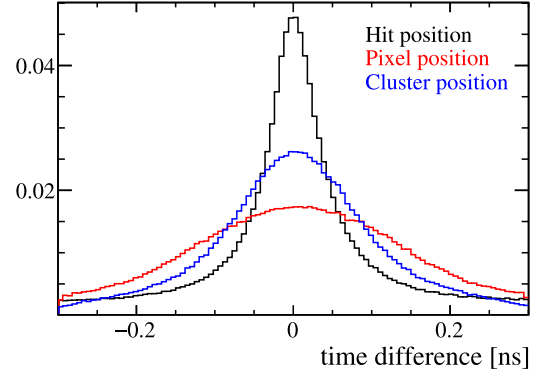


Fig. 3. Resolution on the photon emission time from the photon reconstruction. Three configurations are shown: using the true hit coordinate as the hit position; using the pixel centre as the hit position; and using the cluster centre as the pixel centre.

derived using TORCH information alone. This is achieved by obtaining a likelihood profile for each track as a function of  $t_{\text{arrival}}$  and combining the likelihood of all the tracks associated with the same vertex. However, the VELO detector for LHCb Upgrade II is expected to provide fast timing in a small region around the vertex. Therefore, it is also possible to use such information as a source for  $t_0$ . The TOF is computed as  $d_{\text{track}}/(\beta c)$ , where  $d_{\text{track}}$  is the path length of the charged particle, computed via interpolation from the positions measured by the tracking system, and  $\beta$  is computed for the hypothesis under consideration for the particle mass ( $\pi$ ,  $K$  or  $p$ ). The propagation time of the photon can be computed from its path length in the TORCH as  $t_{\text{prop}} = d_{\text{prop}}/v_{\text{group}}$ , where  $v_{\text{group}}$  is the group velocity, which depends on photon energy. The dependence of the quartz refractive index on photon energy leads to chromatic dispersion. Photons with different energies produced by the same track will be emitted with different Cherenkov angles, as can be seen in Fig. 1. As a consequence, the Cherenkov angle can be used to correct for the chromatic dispersion. This is essential in TORCH to cover the momentum range of interest and leads to a different reconstruction approach in TORCH compared to e.g. the Belle II TOP [5].

In order to compute the Cherenkov angles and path length, the photon path is reconstructed by associating the detected position at the MCP-PMT with charged hadrons traversing the quartz radiator bars. This reconstruction is done via an analytical back-propagation. In this process the exact path is unknown and the properties are evaluated for different combinations of reflections on the sides and the bottom of the module for each photon-track pair. There is also an ambiguity about where the Cherenkov photon is emitted and it is assumed that each photon is produced at the centre of the radiator. These assumptions introduce an implicit resolution on the photon emission time, as can be seen in Fig. 3.

The aim is to obtain the probability of a given hit being produced by a track/hypothesis. This is achieved by combining all the aforementioned information in the probability density function (PDF) for each track/photon/hypothesis combination. At the photon emission point, the PDF depends on  $t_0$ , the photon energy (or equivalently  $\theta_c$ ),  $\phi_c$  and  $z$  (aligned with the LHC beam pipe). The considered hypothesis and number of lateral reflections are encoded in the Cherenkov angles. The variables factorize such that

$$\begin{aligned} P(E_\gamma, \phi_c, z, t_0) &= P(E_\gamma)P(\phi_c)P(z)P(t_0)\Theta(E_\gamma, \phi_c, z) \\ &= \frac{1}{2\pi} \frac{1}{r_z} P(E_\gamma)P(t_0)\Theta(E_\gamma, \phi_c, z). \end{aligned} \quad (2)$$

The function  $\Theta(E_\gamma, \phi_c, z)$  is a step function that is equal to one if a photon is able to be successfully mapped to the detector plane and zero otherwise. The resolution in time due to the electronics can be translated to a Gaussian smearing of  $t_0$ . The PDF describing the emission is normalized by Monte Carlo integration. The PDF on the

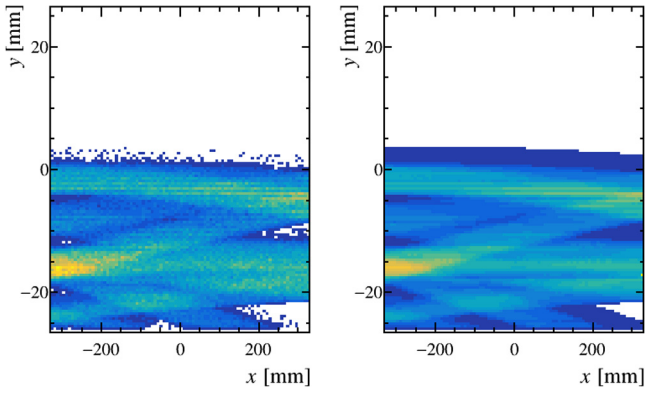


Fig. 4. Comparison between the image from a single track obtained (left) by forward mapping  $10^6$  photons through the TORCH optics and (right) from  $P(\vec{x}'')$  shown integrated over time.

detector plane is given by  $P(x_d'', y_d'', t_d)$ , where  $x_d'', y_d'', t_d$  are the spatial and temporal coordinates in the detector plane. This is related to the initial PDF by a transformation. Since  $x_d''$  and  $y_d''$  are independent of  $t_0$ , the determinant of the Jacobian matrix for the transformation is given by

$$|J| = \left| \frac{\partial y_d''}{\partial E_\gamma} \frac{\partial x_d''}{\partial \phi c} - \frac{\partial x_d''}{\partial E_\gamma} \frac{\partial y_d''}{\partial \phi c} \right|, \quad (3)$$

The derivatives can be computed numerically, by mapping four photons through the optics, or analytically. Because the image is three dimensional, and very fine grained in space and time, it is not practical to approximate the PDF numerically by ray-tracing photons through the TORCH optics. However, such numerical approximation can be used as a cross-check. The PDF evaluated for a single track is compared to the pattern expected from mapping a large number of photons from the track through the TORCH optics in Fig. 4. The same features are reproduced by both approaches.

The log-likelihood for a given track,  $t$ , and hypothesis,  $h_t$ , is given by

$$\log L = \sum_{\text{pixel } i} \log \left( \frac{N_i}{N_{\text{tot}}} P_i(\vec{x}_i'' | h_t) + \sum_{\text{track } j} \frac{N_j}{N_{\text{tot}}} P_j(\vec{x}_i'' | h_j^{\text{best}}) + \frac{N_{\text{bkg}}}{N_{\text{tot}}} P_{\text{bkg}}(\vec{x}_i'') \right), \quad (4)$$

where  $h_j^{\text{best}}$  is the best guess of the particle mass hypothesis for track  $j$ , and  $P_{\text{bkg}}(\vec{x}_i'')$  is the PDF describing the background from photons not associated with reconstructed particles. The background PDF is assumed to be uniformly distributed in space and time. The ratio of photons associated to each component,  $N_j/N_{\text{tot}}$ , is estimated by propagating 1000 photons per track through the TORCH optics. These fractions are fixed in the likelihood fit as finding the yields in a fit is not practical. The ‘best’ hypothesis for each particle is determined in an iterative manner. First all tracks are assigned the pion hypothesis as the ‘best’ hypothesis. For each track the log-likelihood for each hypothesis ( $\pi$ ,  $K$ ,  $p$ ) is then evaluated. Each track is then assigned its best working hypothesis, defined as the one that maximizes the log-likelihood. This process is then repeated a number of times, with  $h_j^{\text{best}}$  set to be the best hypothesis from the previous iteration. This process converges quickly and only three iterations are used. This is the same approach used in the LHCb RICH detectors [6]. The likelihood calculation only considers tracks in the same module as each module is optically isolated.

### 3. Performance

In order to estimate the impact of TORCH on LHCb’s PID performance, the TORCH detector is added to the LHCb GEANT4 simulation

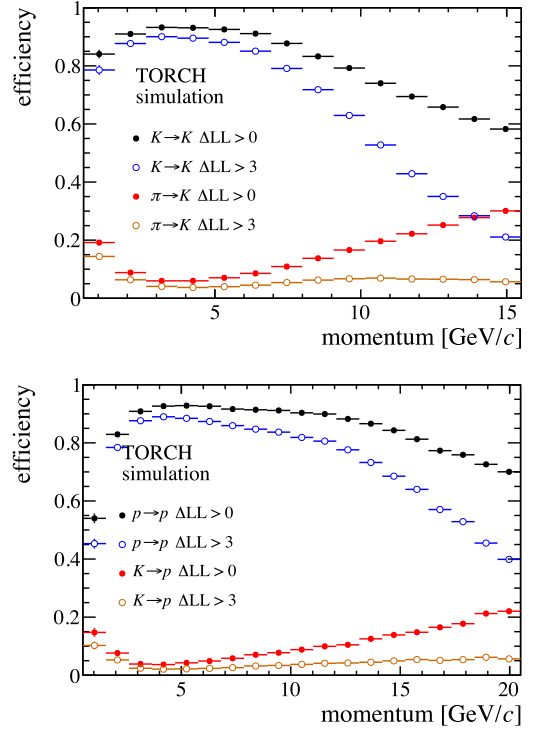


Fig. 5. TORCH PID performance in LHCb in high luminosity LHC data taking conditions. Two different likelihood requirements are shown for kaon-pion separation efficiency (top) and for proton-kaon separation efficiency (bottom).

[7–9]. High-luminosity LHC conditions, corresponding to those expected during the Run 4 of the LHC ( $\mathcal{L} = 1.4 \times 10^{34} \text{ cm}^{-2} \text{ s}^{-1}$ ), are simulated. The ability to separate pions and protons from kaons at lower momentum, with the aforementioned conditions, is demonstrated in Fig. 5, where a selection based on the likelihood ratio between different particle identification hypotheses is used. As can be seen, good separation between kaons and pions is achieved below momentum of 10 GeV/c and between kaons and protons up to about 15 GeV/c momentum. These momentum regions complement the PID provided by the RICH detectors and thus TORCH has great potential to improve the physics reach of the LHCb experiment.

With Run 4 conditions, the reconstruction algorithm takes  $\mathcal{O}(1\text{s})$  per event.<sup>1</sup> Although significant effort has been put into reducing this time further optimization is still needed. In order to fit the time budget of the LHCb trigger system, the full event reconstruction of TORCH needs to be completed in  $\mathcal{O}(10 \text{ ms})$ . Several bottlenecks and under-performing calculations have already been identified and future versions of the code will include improvements on these aspects. The likelihood calculation is well suited for parallelization as each module is completely independent and the probabilities for a given hit/track/hypothesis combination could be determined independently. As a consequence, a significant speed-up could be possible by using accelerator platforms such as GPUs and IPU. Motivated by this, the TORCH photon mapping has been developed for these platforms as a proof-of-principle. Additionally, a *local* likelihood can be computed by

<sup>1</sup> Tested using a Intel Core i5-10500 3.10 GHz.

removing the second term in Eq. (4). This approach considers each hadron in isolation and, thus, no iteration is needed and it is more parallelizable. The downside is that the background is sub-optimally reproduced. However, considering that there is already a large background due to photons not associated to any reconstructed track, the performance is not significantly affected with respect to the previously described approach.

#### 4. Conclusions

TORCH is a large scale time-of-flight detector aiming to provide charged particle separation in the 2–15 GeV/ $c$  momentum range over a 9.5 m flight path. Adding PID capability in the lower momentum region, it has potential to significantly improve sensitivity across the wide physics programme of the LHCb experiment. Simulations of the TORCH detector show that it has the ability to significantly enhance the particle identification capabilities in this momentum region. The improved particle identification capability delivered by TORCH will have many applications in the LHCb physics programme. The biggest gains are expected in channels with protons (including measurements of pentaquark states) or soft-particles. The latter will increase the uniformity over phase space of amplitude analyses and could significantly improve the flavour-tagging performance of the detector (increasing the effective sample size of  $CP$ -violation measurements). TORCH will also provide opportunities for analyses with deuterons and other heavy charged particles.

#### Declaration of competing interest

The authors declare that they have no known competing financial interests or personal relationships that could have appeared to influence the work reported in this paper.

#### Acknowledgements

The support is acknowledged of the Science and Technology Research Council, UK, grant number ST/P002692/1, of the European Research Council through an FP7 Advanced Grant (ERC-2011-AdG 299175-TORCH) and of the Royal Society, UK.

#### References

- [1] R. Calabrese, et al., Performance of the LHCb RICH detectors during LHC Run2, *J. Instrum.* 17 (07) (2022) P07013, <http://dx.doi.org/10.1088/1748-0221/17/07/P07013>.
- [2] M.J. Charles, R. Forty, TORCH: Time of flight identification with cherenkov radiation, *Nucl. Instrum. Methods A* 639 (2011) 173–176, <http://dx.doi.org/10.1016/j.nima.2010.09.021>.
- [3] LHCb Collaboration, Framework TDR for the LHCb Upgrade II - Opportunities in Flavour Physics, and Beyond, in the HL-LHC Era, CERN, Geneva, 2021, <http://cds.cern.ch/record/2776420>.
- [4] T.M. Conneely, et al., The TORCH PMT: A close packing, multi-anode, long life MCP-PMT for Cherenkov applications, *JINST* 10 (5) (2015) C05003, <http://dx.doi.org/10.1088/1748-0221/10/05/C05003>.
- [5] U. Tamponi, The TOP counter of belle II: Status and first results, *Nucl. Instrum. Methods Phys. Res. A* 952 (2020) 162208, <http://dx.doi.org/10.1016/j.nima.2019.05.049>, 10th International Workshop on Ring Imaging Cherenkov Detectors (RICH 2018).
- [6] R.W. Forty, O. Schneider, RICH Pattern Recognition, Tech. Rep., (LHCb-98-040) CERN, 1998, <http://cds.cern.ch/record/684714>.
- [7] S. Agostinelli, et al., Geant4: A simulation toolkit, *Nucl. Instrum. Meth. A506* (2003) 250, [http://dx.doi.org/10.1016/S0168-9002\(03\)01368-8](http://dx.doi.org/10.1016/S0168-9002(03)01368-8).
- [8] J. Allison, K. Amako, J. Apostolakis, H. Araujo, P. Dubois, et al., Geant4 developments and applications, *IEEE Trans. Nucl. Sci.* 53 (2006) 270, <http://dx.doi.org/10.1109/TNS.2006.869826>.
- [9] M. Clemencic, et al., The LHCb simulation application, Gauss: Design, evolution and experience, *J. Phys. Conf. Ser.* 331 (2011) 032023, <http://dx.doi.org/10.1088/1742-6596/331/3/032023>.